ISSN 1070-3284, Russian Journal of Coordination Chemistry, 2014, Vol. 40, No. 12, pp. 904–910. © Pleiades Publishing, Ltd., 2014.

Ionothermal Synthesis of Two Chiral Three-Dimensional Metal-Organic Frameworks Based on D-Camphoric Acid[1]

L. Li, S. Chen, Y. J. Ning, Y. Bai*, and D. B. Dang**

Henan Key Laboratory of Polyoxometalate Chemistry, Institute of Molecular and Crystal Engineering, College of Chemistry and Chemical Engineering, Henan University, Kaifeng, 475004 P.R. China

e-mail: baiyan@henu.edu.cn; dangdb@henu.edu.cn***

Received April 28, 2014

Abstract—Two three-dimensional chiral metal-organic frameworks [PMIm][Co_2(D-Cam)$_2$(CH_3COO)] (**I**) and [BMIm][Mn_2(D-Cam)$_2$(CH_3COO)] · H_2O (**II**) (PMIm = 1-propyl-3-methylimidazolium, BMIm = 1-butyl-3-methylimidazolium, D-Cam = D-camphoric acid) have been synthesized under the ionothermal conditions and structurally characterized by IR spectroscopy, elemental analysis, XRPD, and X-ray single-crystal structure analysis (CIF files CCDC nos. 979650 (**I**) and 979649 (**II**)). Two structures exhibit similar three-dimentional frameworks constructed by the coordination interactions of binuclear metal secondary building units and two bridging ligands of D-Cam and CH_3COO^-, in which $[PMIm]^+$ cations for **I** and $[BMIm]^+$ cations for **II** as templates are filled in the void of frameworks.

DOI: 10.1134/S1070328414120082

INTRODUCTION

The science of metal-organic frameworks (MOFs) with multitopic organic linkers and metal nodes is an area of great interest owing to their potential to exhibit structure-dependent behavior, such as magnetic, optical, catalytic and adsorbent properties [1–5]. So far, investigations have mainly involved the construction of MOFs under hydrothermal, solvothermal conditions or room-temperature crystallization [6]. In contrast, the use of ionic liquids (ILs) in the design and synthesis of MOFs has been much less explored, despite their excellent properties including the low melting points, low vapor pressure, high thermal stability, ionic conductivity, and their abilities to dissolve a wide range of organic and inorganic compounds [7–9]. In the coordination chemistry-based self-assembly, ionic liquids can be functioned as reaction media and structure templates, which may result in a rich diversity of microarchitectures and topologies [10–13].

As an important part of MOFs, chiral MOFs are of particular interest showing promise in not only the intriguing variety of architectures and topologies, but also their applications such as in nonlinear optics, enantiomerically selective catalysis and separation [14–16]. An efficient strategy constructing chiral MOFs is the incorporation of enantiopure organic ligands. D-camphoric acid (D-Cam), as a kind of chiral ligands, has comparatively small volume and versatile coordination behavior. A series of homochiral MOFs based on D-Cam have been reported via hydrothermal synthesis [17–20], however, homochiral MOFs synthesized in ILs are relatively few [21]. In 2008, Xianhui Bu reports a homochiral framework (EMIm)[Co_2(D-Cam)$_2$(Ac)] (EMIm = 1-ethyl-3-methylimidazolium, Ac = acetate) through ionothermal synthesis [22]. As part of our continuing investigations on the construction of functional MOFs [14, 17, 23, 24], herein we have successfully synthesized two 3D chiral metal-organic frameworks [PMIm][Co_2(D-Cam)$_2$(CH_3COO)] (I) and [BMIm][Mn_2(D-Cam)$_2$(CH_3COO)] · H_2O (II) through the use of [PMIm]Br (1-propyl-3-methylimidazolium bromide) and [BMIm]Br (1-butyl-3-methylimidazolium bromide) as solvents.

EXPERIMENTAL

All chemicals were of reagent grade quality obtained from commercial sources and used without further purification. [PMIm]Br and [BMIm]Br were prepared according to the literature method [25]. Elemental analyses (C, H, and N) were carried out on a PerkinElmer 240C analytical instrument. IR spectra were recorded from KBr pellets with a Nicolet 170 SXFT-IR spectrophotometer in the 4000–400 cm^{-1} region. Powder X-ray diffraction patterns were recorded on a D/max-g A rotating anode X-ray diffractometer with a sealed Cu tube (λ = 1.54178 Å).

Synthesis of complex I. A mixture of $Co(CH_3COO)_2 \cdot 4H_2O$ (0.37 g, 1.5 mmol), D-Cam (0.20 g, 1.0 mmol), and [PMIm]Br (1.80 g, 8.8 mmol) in a 25 mL Teflon-lined stainless-steel autoclave was heated to 120°C for 5 days in a furnace. The resulting mixture was naturally cooled to get purple crystals of **I**

[1] The article is published in the original.

suitable for single-crystal X-ray diffraction. The total yield was 60% based on D-Cam.

For $C_{29}H_{44}N_2O_{10}Co_2$ ($M = 698.53$)

anal. calcd., %:	C, 49.86;	H, 6.35;	N, 4.01.
Found, %:	C, 49.77;	H, 6.31;	N, 3.95.

IR (KBr; ν, cm^{-1}): 3428 m, 3143 w, 3103 w, 3052 w, 2967 m, 2928 w, 2881 w, 1630 s, 1566 s, 1448 m, 1401 v.s, 1364 m, 1291 w, 1175 m, 1130 w, 799 w, 782 w.

Synthesis of complex II was carried out in a similar manner to that of I, except that [BMIm]Br (1.80 g) was used instead of [PMIm]Br, $Mn(CH_3COO)_2 \cdot 4H_2O$ (0.37 g, 1.5 mmol) instead of $Co(CH_3COO)_2 \cdot 4H_2O$. The yellow crystals of **II** are suitable for single-crystal X-ray diffraction. The total yield was 71% based on D-Cam.

For $C_{30}H_{48}N_2O_{11}Mn_2$ ($M = 722.59$)

anal. calcd., %:	C, 49.87;	H, 6.70;	N, 3.88.
Found, %:	C, 49.81;	H, 6.62;	N, 3.94.

IR (KBr; ν, cm^{-1}): 3455 m, 3154 w, 3091 w, 3060 m, 2964 m, 2938 w, 2877 w, 1627 s, 1552 s, 1460 m, 1401 v.s, 1365 m, 1319 m 1291 w, 1175 m, 1129 w, 798 m, 784 m.

X-ray crystallography. A suitable crystal of size $0.17 \times 0.13 \times 0.09$ mm for **I** and $0.25 \times 0.22 \times 0.18$ mm for **II** were chosen for the crystallographic study and mounted on a Bruker Smart APEX II CCD diffractometer. All diffraction measurements were performed at room temperature using graphite-monochromatized MoK_α radiation ($\lambda = 0.71073$ Å). The structure was solved by Direct Methods and refined on F^2 by using full-matrix least-squares methods with the SHELXL-97 program [26, 27]. Space group, lattice parameters and other relevant information are listed in Table 1 and selected bond lengths and angles are given in Table 2.

Supplementary material has been deposited with the Cambridge Crystallographic Data Centre (nos. 979650 (**I**) and 979649 (**II**); deposit@ccdc.cam.ac.uk or http://www.ccdc.cam.ac.uk).

RESULT AND DISCUSSION

The IR spectra of complexes **I** and **II** give clear evidences of characteristic bands of carboxylates. The bands at 1566, 1401 cm^{-1} for **I** and 1552, 1401 cm^{-1} for **II** show the antisymmetric and symmetric stretching vibrations of COO^- [28, 29]. The peaks from 3052 to 3143 cm^{-1} for **I** and 3060 to 3154 cm^{-1} for **II** should be attributed to the stretching vibrations of C–H for imidazolium. The bands at 2967 cm^{-1} for **I** and 2964 cm^{-1} for **II** are assigned to C–H stretching vibrations of methyl and methylene [30]. These results were finally confirmed by X-ray crystallography.

Table 1. Crystallographic data and refinement parameters for complexes of **I** and **II**

Parameter	Malue	
	I	**II**
Formula weight	698.52	722.58
Temperature, K	295(2)	296(2)
Crystal system	Orthorhombic	Orthorhombic
Space group	$P2_12_12_1$	$P2_12_12_1$
a, Å	13.3950(8)	13.085(6)
b, Å	13.5119(8)	14.106(7)
c, Å	17.6200(10)	18.175(9)
V, Å^3	3189.1(3)	3354(3)
Z	4	4
ρ_{calcd}, g cm^{-3}	1.455	1.431
μ, mm^{-1}	1.097	0.812
$F(000)$	1464	1520
θ Range for data collection, deg	1.90–25.00	1.83–24.99
Scan mode	ω	ω
Number of unique reflections (N_1)	5611 ($R_{int} = 0.0519$)	5905 ($R_{int} = 0.0388$)
Number of reflections with $I > 2\sigma(I)$ (N_2)	4081	4967
Number of parameters refined	388	424
GOOF (F^2)	1.079	1.058
R_1 for N_2	0.0539	0.0360
wR_2 for N_1	0.1577	0.0994
$\Delta\rho_{max}/\Delta\rho_{min}$, e Å^{-3}	0.966/–0.386	0.280/–0.400

Table 2. Selected bond lengths (Å) and bond angles (deg) of **I***

Bond	*d*, Å	Bond	*d*, Å
		I	
Co(1)–O(2)	2.044(5)	Co(2)–O(1)	2.035(5)
Co(1)–O(3*A*)	2.049(5)	Co(2)–O(4*A*)	2.039(5)
Co(1)–O(5*B*)	2.037(5)	Co(2)–O(6*B*)	2.039(5)
Co(1)–O(8)	2.014(5)	Co(2)–O(7)	2.033(5)
Co(1)–O(10*C*)	2.002(4)	Co(2)–O(9)	2.023(4)
		II	
Mn(1)–O(1)	2.098(2)	Mn(2)–O(2)	2.126(3)
Mn(1)–O(3*A*)	2.133(3)	Mn(2)–O(4*A*)	2.101(3)
Mn(1)–O(6*B*)	2.110(3)	Mn(2)–O(5*B*)	2.093(3)
Mn(1)–O(8)	2.084(3)	Mn(2)–O(7)	2.142(3)
Mn(1)–O(9)	2.070(3)	Mn(2)–O(10*C*)	2.070(2)
Angle	ω, deg	Angle	ω, deg
		I	
O(2)Co(1)O(3*A*)	88.5(2)	O(5*B*)Co(1)O(2)	89.2(2)
O(8)Co(1)O(2)	159.6(2)	O(10*C*)Co(1)O(2)	97.0(2)
O(5*B*)Co(1)O(3*A*)	164.00(19)	O(8)Co(1)O(3*A*)	88.7(2)
O(10*B*)Co(1)O(3*A*)	99.8(2)	O(8)Co(1)O(5*B*)	87.9(2)
O(10*C*)Co(1) O(5*B*)	96.2(2)	O(10*C*)Co(1)O(8)	103.4(2)
O(1)Co(2)O(4*A*)	88.4(2)	O(1)Co(2)O(6*B*)	89.6(2)
O(7)Co(2)O(1)	164.3(2)	O(9)Co(2)O(1)	101.34(19)
O(7)Co(2)O(4*A*)	87.5(2)	O(9)Co(2)O(4*A*)	97.0(2)
O(4*A*)Co(2)O(6*B*)	160.33(19)	O(7)Co(2)O(6*B*)	89.1(2)
O(9)Co(2)O(6*B*)	102.62(18)	O(9)Co(2)O(7)	94.2(2)
		II	
O(1)Mn(1)O(3A)	87.80(11)	O(1)Mn(1)O(6*B*)	88.86(12)
O(8)Mn(1)O(1)	155.06(12)	O(9)Mn(1)O(1)	97.67(11)
O(6*B*)Mn(1)O(3*A*)	158.05(12)	O(8)Mn(1)O(3*A*)	87.47(11)
O(9)Mn(1)O(3A)	102.31(12)	O(8)Mn(1)O(6*B*)	86.47(12)
O(9)Mn(1)O(6*B*)	99.63(12)	O(9)Mn(1)O(8)	107.27(11)
O(4*A*)Mn(2)O(2)	86.25(11)	O(5B)Mn(2)O(2)	88.75(12)
O(2)Mn(2)O(7)	158.83(12)	O(10*C*)Mn(2)O(2)	100.71(11)
O(5*B*)Mn(2)O(4*A*)	156.03(12)	O(4*A*)Mn(2)O(7)	86.78(11)
O(10*C*)Mn(2)O(4*A*)	101.99(11)	O(10*C*)Mn(2)O(5*B*)	101.97(11)
O(5*B*)Mn(2)O(7)	89.55(12)	O(10*C*)Mn(2)O(7)	100.29(11)

* Symmetry codes: (*A*) $0.5 + x$, $3.5 - y$, $3 - z$; (*B*) $-0.5 + x$, $2.5 - y$, $3 - z$; (*C*) $2.5 - x$, $3 - y$, $-0.5 + z$ for **I**.

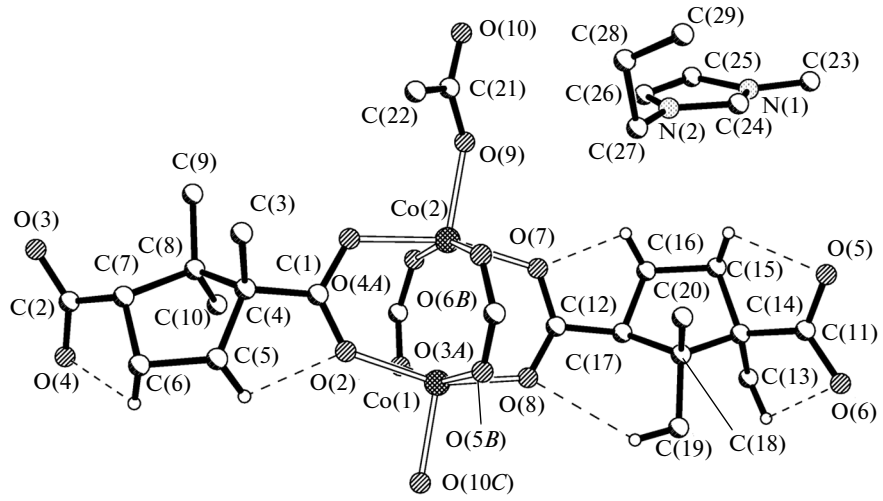

Fig. 1. The structure of **I** and the coordination environment of Co(1) and Co(2) centers showing hydrogen bonds with dashed line (symmetry codes: (*A*) $0.5 + x$, $3.5 - y$, $3 - z$; (*B*) $-0.5 + x$, $2.5 - y$, $3 - z$; (*C*) $2.5 - x$, $3 - y$, $-0.5 + z$).

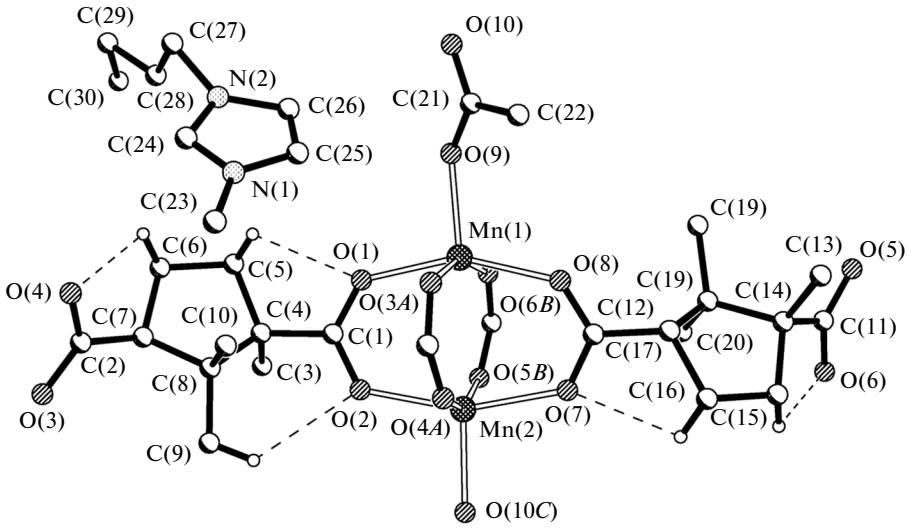

Fig. 2. The structure of **II** and the coordination environment of Mn(1) and Mn(2) centers showing hydrogen bonds with dashed line (symmetry codes: (*A*) $0.5 + x$, $1.5 - y$, $1 - z$; (*B*) $-0.5 + x$, $0.5 - y$, $1 - z$; (*C*) $2.5 - x$, $1 - y$, $0.5 + z$).

Single-crystal X-ray diffraction analysis has revealed that both **I** and **II** exhibit crystalline 3D metal-organic frameworks constructed by the coordination interactions of binuclear metal secondary building units (SBUs) and two bridging ligands (D-Cam and CH_3COO^-) with $[PMIm]^+$ cations for **I**, $[BMIm]^+$ cations for **II** as templates. The coordination environment of the metal atoms is depicted in Fig. 1 and Fig. 2, respectively. Each metal atom has a distorted square pyramid geometry and is coordinated by five oxygen atoms from four D-Cam anions ((Co(1): O(2) and O(3*A*) of Cam-1, O(5*B*) and O(8) of Cam-2; Co(2): O(1) and O(4*A*) of Cam-1, O(6*B*) and O(7) of Cam-2)) and one CH_3COO^- anion (O(10*C*) for Co(1) and O(9) for Co(2)). In complex **II**, the oxygen donors are O(1) and O(3*A*) of Cam-1, O(6*B*) and O(8) of Cam-2, O(9) of CH_3COO^- anion for Mn(1), O(2) and O(4*A*) of Cam-1, O(5*B*) and O(7) of Cam-2, O(10*C*) of CH_3COO^- for Mn(2). The M–O distances are in the range of 2.002(4)–2.049(5) Å for Co–O and 2.070(2)–2.142(3) Å for Mn–O. Four carboxylate groups from two Cam-1 and two Cam-2 ligands bridge M(1) and M(2) centers to form a paddle-wheel $\{M_2O_{10}C_4\}$ as SBU with a M···M separation of 2.85 Å for **I** and 3.04 Å for **II**, respectively.

Each SBU is interconnected with four SBUs along multi-direction through the modes of SBU-Cam-SBU and SBU-CH_3COO-SBU. Cam-1 is one of

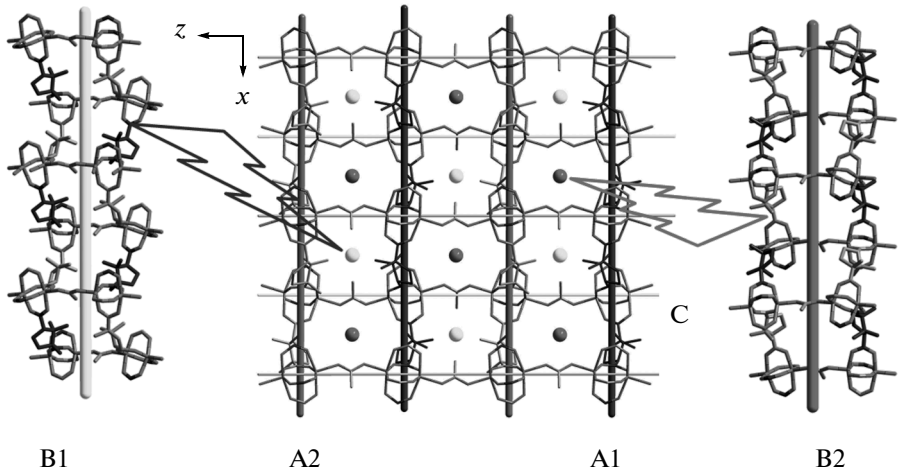

Fig. 3. View of 3D structure in **I** and **II**. The $[PMIm]^+$ cations for I and $[BMIm]^+$ cations and water molecules for **II** have been omitted.

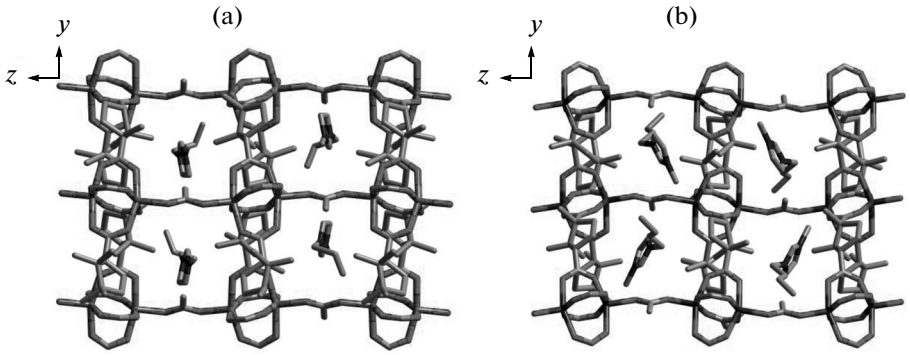

Fig. 4. View of **I** (a) and **II** (b) containing $[PMIm]^+$ and $[BMIm]^+$ cations, respectively. The hydrogen atoms and water molecules have been omitted for clarity.

SBUs' linkers (SBU-Cam1-SBU), which enables infinite prolongation of SBUs in the form of 2_1 right-handed helical chains along *x* orientation with the pitch length of 13.3950(8) Å for **I** and 13.085(6) Å for **II**, respectively (Fig. 3, A1). Cam-2 is coordinated to the adjacent SBUs in the mode of SBU-Cam2-SBU, forming a 2_1 left-handed helical chain along *x* orientation (Fig. 3, A2). Otherwise, the adjacent SBUs connected by CH_3COO^- anions in the mode of SBU-CH_3COO-SBU, form a helical chain along *z* orientation with the pitch length of 17.6200(10) Å for **I** and 18.175(9) for **II**, respectively (Fig. 3, C). The cross-linking of adjacent SBUs connected by the modes of SBU-Cam-SBU and SBU-CH_3COO-SBU leads to a grid-like (4,4) layer substructure along the *xz* plane. The adjacent Cam-1 and Cam-2 are connected by SBUs in the mode of cam1-SBU-Cam2 along *y* axis, constructing a three-dimensional framework, in which two 2_1 double helical chains can be found with the pitch lengths of 13.5119(8) Å for **I** and 14.106(7) Å for **II** (the length of the crystallographic *y* axis) (Fig. 3, B1, B2). Therefore, the resulting three-dimensional frameworks of complexes **I** and **II** are formed by stretching the helices and they are homochiral owing to the presence of the enantiopure building block [17]. The three-dimensional chiral frameworks **I** and **II** display similar channels, in which the trapped inside the voids $[PMIm]^+$ for **I**, $[BMIm]^+$ and water molecules for **II** have a great influence on structure in the solid state (Fig. 4). In addition, several hydrogen bonds can be found in three-dimensional networks, which play an important role in stabilizing the 3D structures (Table 3).

The X-ray powder diffraction (XRPD) measurements were performed for **I** and **II**. The experimental XRPD patterns of the two complexes are quite similar to those calculated from their single-crystal X-ray data, indicating that the bulk products of **I** and **II** are both pure phase. The intensity difference between experimental and simulated XRPD patterns is due to the variation in preferred orientation of the powder sample during collection of the experimental XRPD.

Table 3. Geometric parameters of hydrogen bonds for **I** and **II**

D-H···A	Distance, Å				Symmetry codes of atom A
	D–H	H···A	D···A	angle DHA, deg	
I					
C(5)–H(5*B*)···O(2)	0.97	2.22	2.683(10)	108	
C(6)–H(6A)···O(4)	0.97	2.43	2.834(9)	104	
C(13)–H(13C)···O(6)	0.96	2.42	2.749(10)	100	
C(15)–H(15*A*)···O(5)	0.97	2.36	2.755(8)	103	
C(16)–H(16*B*)···O(7)	0.97	2.39	2.864(10)	108	
C(19)–H(19*A*)···O(8)	0.96	2.52	3.196(10)	127	
C(22)–H(22*B*)···O(6)	0.96	2.52	3.352(8)	146	$-0.5 + x, 2.5 - y, 3 - z$
C(24)–H(24*A*)···O(10)	0.93	2.46	3.294(15)	148	$3 - x, -0.5 + y, 3.5 - z$
II					
O(1*w*)–H(1*wC*)···O(1)	0.85	2.43	3.193(8)	150	$2 - x, 0.5 + y, 0.5 - z$
O(1*w*)–H(1*wD*)···O(9)	0.85	2.07	2.833(7)	148	$2 - x, 0.5 + y, 0.5 - z$
C(5)–H(5*A*)···O(1)	0.97	2.37	2.728(5)	101	
C(6)–H(6*B*)···O(4)	0.97	2.41	2.843(5)	107	
C(9)–H(9*B*)···O(2)	0.96	2.58	3.186(6)	121	
C(15)–H(15*A*)···O(6)	0.97	2.31	2.754(5)	107	
C(16)–H(16*B*)···O(7)	0.97	2.42	2.830(5)	105	
C(22)–H(22*A*)···O(2)	0.96	2.51	3.304(5)	140	$2.5 - x, 1 - y, -0.5 + z$
C(24)–H(24*A*)···O(10)	0.93	2.27	3.189(7)	169	$2 - x, 0.5 + y, 0.5 - z$

ACKNOWLEDGMENTS

This work was supported by the Natural Science Foundation of Henan Province of China, the Foundation of the Education Department of Henan Province of China and the Foundation of Henan University cosponsored by Henan Province and Ministry of Education of China.

REFERENCES

1. Katsoulidis, A.P., Park, K.S., Antypov, D., et al., *Angew. Chem. Int. Ed.*, 2014, vol. 53, p. 193.
2. Kong, G.Q., Han, Z.D., He, Y.B., et al., *Chem. Eur. J.*, 2013, vol. 19, p. 14886.
3. Huang, Y.L., Gong, Y.N., Jiang, L., et al., *Chem. Commun.,* 2013, vol. 49, p. 1753.
4. Zhao, J.P., Han, S.D., Zhao, R., et al., *Inorg. Chem.*, 2013, vol. 52, p. 2862.
5. Wang, Y., Yang, J., Liu, Y., et al., *Chem. Eur. J.*, 2013, vol. 19, p. 14591.
6. Stock, N. and Biswas, S., *Chem. Rev.*, 2012, vol. 121, p. 933.
7. Meng, Y., Liu, J.L., Zhang, Z.M., et al., *Dalton Trans.*, 2013, vol. 42, p. 12853.
8. Liu, Q.Y., Li, Y.L., Wang, Y.L., et al., *CrysEngComm*, 2014, vol. 16, p. 486.
9. Tan, B., Xie, Z.L., Feng, M.L., et al., *Dalton Trans.*, 2012, vol. 41, p. 10576.
10. Lin, Z.J., Wragg, D.S., Warren, J.E., et al., *J. Am. Chem. Soc.*, 2007, vol. 129, p. 10334.
11. Zhan, C.H., Wang, F., Kang, Y., et al., *Inorg. Chem.*, 2012, vol. 51, p. 523.
12. Li, S.Y., Wang, W., Liu, L., et al., *CrystEngComm,* 2013, vol. 15, p. 6424.
13. Wei, Y., Marler, B., Zhang, L., et al., *Dalton Trans.*, 2012, vol. 41, p. 12408.
14. Dang, D.B., Wu, P.Y., He, C., et al., *J. Am. Chem. Soc.*, 2010, vol. 132, p. 14321.
15. Yoon, M., Srirambalaji, R., and Kim, K., *Chem. Rev.*, 2012, vol. 112, p. 1196.
16. Li, J.R., Sculley, J., and Zhou, H.C., *Chem. Rev.*, 2012, vol. 112, p. 869.
17. Dang, D.B., An, B., Bai, Y., et al., *Chem. Commun.,* 2013, vol. 49, p. 2243.

18. Chen, N., Li, M.X., Yang, P., et al., *Cryst. Growth Des.*, 2013, vol. 13, p. 2650.
19. Liang, X.Q., Li, D.P., Zhou, X.H., et al., *Cryst. Growth Des.*, 2009, vol. 9, p. 4872.
20. Zeng, M.H., Wang, B., Wang, X.Y., et al., *Inorg. Chem.*, 2006, vol. 45, p. 7069.
21. Liu, Q.Y., Xiong, W.L., Liu, C.M., et al., *Inorg. Chem.*, 2013, vol. 52, p. 6773.
22. Chen, S.M., Zhang, J., and Bu, X.H., *Inorg. Chem.,* 2008, vol. 47, p. 5567.
23. Bai, Y., Wang, J.L., Dang, D.B., et al., *CrystEngComm*, 2012, vol. 14, p. 1575.
24. Bai, Y., Gao, H., Dang, D.B., et al., *CrystEngComm*, 2010, 12, p. 1422.
25. Parnham, E.R. and Morris, R.E., *Chem. Mater.,* 2006, vol. 18, p. 4882.
26. Sheldrick, G.M., *Acta Crystallogr., A,* 1990, vol. 46, p. 467.
27. Sheldrick, G.M., *Acta Crystallogr., A,* 2008, vol. 64, p. 112.
28. Chen, N., Yang, P., He, X., et al., *Inorg. Chim. Acta,* 2013, vol. 405, p. 43.
29. Wilson, J.A. and LaDuca, R.L., *Inorg. Chim. Acta,* 2013, vol. 403, p. 136.
30. Xu, L., Choi, E.Y., and Kwon, Y.U., *Inorg. Chem.*, 2007, vol. 46, p. 10670.